CASE REPORT

Myelopathy secondary to an intramedullary arteriovenous malformation in a mature dog

Maria Ines De Freitas[1] [ID] | Daniel Housley[1] | Abby Caine[1] | Emilie Fauchon[1] | Kerstin Baiker[2] | Davide Corbetta[2] | Giunio B Cherubini[1]

[1]Dick White Referrals, Six Mile Bottom, UK

[2]School of Veterinary Medicine and Science, University of Nottingham, Sutton Bonington, UK

Correspondence
Maria Ines De Freitas, Dick White Referrals, Station Farm, London Road, CB80UH Six Mile Bottom, UK.
Email: ines.defreitas@dwr.co.uk

Abstract

A 2-year-old crossbreed dog was presented for evaluation of a 6-week history of progressive paraparesis. Magnetic resonance imaging and computed tomography angiography of the thoracic and lumbar spinal cord disclosed multifocal, anomalous, small, vascular structures, distributed throughout the subarachnoid space of the included section of the spinal cord. An additional focal intramedullary lesion was identified extending from T9 to T10 to T12. Histopathological examination confirmed the presence of an intramedullary arteriovenous malformation affecting the thoracic spinal cord and leading to diffuse congestion and focal hemorrhages into the affected spinal cord.

KEYWORDS

arteriovenous malformation, canine, computed tomography angiography, magnetic resonance imaging, myelopathy, vascular malformation

1 | CASE DESCRIPTION

A 2-year-old, 30 kg, neutered male, crossbreed dog was presented for evaluation of a 6-week history of insidious onset, progressive, non-painful paraparesis. Clinical examination was unremarkable except for moderate muscle atrophy in the pelvic limbs. Neurological examination identified ambulatory paraparesis, proprioceptive ataxia with moderate weakness and proprioceptive deficits in the pelvic limbs, decreased muscle tone and mass in the pelvic limbs, decreased segmental spinal reflexes in the pelvic limbs, intact cutaneous trunci and perineal reflexes, and normal anal tone. Pain was not elicited upon vertebral palpation. There was no history of urinary or fecal incontinence. Hematology and serum biochemistry results were within normal limits.

Abbreviations: AVM, arteriovenous malformation; CT, computed tomography; CTA, computed tomography angiography; FSE, fast spin-echo; GRE, gradient-recalled echo; MRA, magnetic resonance angiography; MRI, magnetic resonance imaging; ST, slice thickness; STIR, short tau inversion recovery; T1W, T1 weighted; T2W, T2 weighted; TE, echo time; TI, inversion time; TR, repetition time; W, weighted.

A diffuse T3-S3 myelopathy was suspected and inflammatory, infectious, congenital, degenerative, and neoplastic diseases were considered.

Magnetic resonance imaging (MRI) was performed using a low-field, 0.4T, permanent, open magnet (Aperto Lucent, Hitachi Medical Corporation, Tokyo, Japan) with an open head coil, to include the thoracolumbar and lumbosacral spinal cord. The patient was positioned in dorsal recumbency with the pelvic limbs in a neutral position and maintained under general anesthesia using a mixture of oxygen, air, and isoflurane. The lumbosacral area was assessed using the following sagittal sequences (slice thickness [ST] 3 mm, matrix 512 × 512, number of signal averages 4): T2-weighted (T2W) fast spin-echo (FSE; repetition time [TR] 2500 ms, echo time [TE] 120 ms), short-tau inversion recovery (STIR; TR 2550 ms, TE 60 ms, inversion time [TI] 100 ms) and T1-weighted (T1W; FSE [TR 532 ms, TE 13 ms]) before and immediately after manual IV injection of gadolinium-based paramagnetic contrast (gadobutrol 1 mmol/mL, 0.1 mL/kg; Bayer plc, Reading, UK). A transverse STIR (TR 5331 ms, TE 60 ms, TI 100 ms)

DE FREITAS ET AL.

Journal of Veterinary Internal Medicine ACVIM

Open Access

American College of
Veterinary Internal Medicine

1099

with 4 mm ST also was acquired between the level of the L4 and L6 vertebrae before contrast administration. When imaging the thoracolumbar area, the following sequences were acquired and evaluated: sagittal T2W FSE (TR 2500 ms, TE 120 ms, ST 3 mm), transverse T2W FSE (TR 5418 ms, TE 100 ms, ST 5 mm), sagittal STIR (TR 2550 ms, TE 60 ms, TI 100 ms, ST 3 mm), transverse T2*-weighted gradient-recalled echo (GRE) sequence (TR 800 ms, TE 27 ms, ST 5 mm), and transverse T1W FSE (TR 745 ms, TE 13 ms, ST 5 mm) before and immediately after manual IV injection of contrast medium as described above.

Evaluation of the MRI by board-certified radiologists identified multifocal, small, well-defined, highly tortuous, signal voiding (T1W and T2W series), moderately contrast-enhancing, tubular structures that were distributed extensively throughout the subarachnoid space within the field of view (arrowheads in Figure 1). These structures were assumed to be vascular with flow-related signal loss. At the level of T11 to T12, a focal, amorphous to ovoid, irregularly marginated, T1W- and T2W-hyperintense (relative to normal spinal cord), strongly enhancing, intramedullary lesion was found, which measured 25 to 28 mm in length and occupied up to 90% of the cross-sectional area of the spinal cord (arrow in Figure 1). Surrounding this intramedullary lesion was a more extensive, poorly delineated, tapering, T2W-hyperintense and T1W-isointense (relative to normal spinal cord), nonenhancing, intramedullary band, which spanned from the level of T9 to T10 to caudal-T12. No magnetic susceptibility artifact was observed within this intramedullary lesion on T2*GRE. The spinal cord had a swollen appearance at the level of this intramedullary lesion.

To further characterize these lesions, MRI was followed by computed tomography angiography (CTA) using a 16-slice multidetector row scanner (MX 8000 IDT, Philips Medical Systems, Cleveland, Ohio). The animal was positioned and maintained under general anesthesia using the same protocol as described above. A volume of helical data was acquired extending from T5 to the sacrum, which was collimated to the vertebral column and reconstructed using bone and soft tissue algorithms with a 1 mm ST. A comparable data set was acquired after IV administration of iodinated contrast (Iohexhol 350 mg I/mL, Omnipaque, General Electric Healthcare at 2 mL/kg) using an automated power injector, with an arterial phase triggered by bolus tracking from the aorta, and a venous phase acquired 60-second postcontrast administration. The CTA confirmed widespread presence of distended, tortuous, occasionally anastomosing, intradural-extramedullary vessels around the periphery of the spinal cord, throughout the field of view (arrowheads in Figure 2). These aberrant vessels showed pronounced enhancement during the arterial phase, which persisted but weakened during the venous phase, suggesting either engorgement of the arterial system or anomalous arterialization of the venous system. By comparison, the major venous drainage routes within the epidural space (including the ventral internal venous plexus and interarcuate veins) and the venous system external to the vertebral canal (including basivertebral veins, intercostal veins, azygous vein, and caudal vena cava) all were determined to be macroscopically normal during CTA. The intramedullary focus at T11 to T12 was better characterized during CTA as a complex vascular plexus, with similar dimensions as observed on MRI, innumerable small tortuous and anastomotic vessels, with strongest enhancement noted during the arterial phase (arrow in Figure 2). Feeding of this intramedullary plexus from the ventral spinal artery cranially was considered most likely, but could not be confirmed.

Based on imaging features and clinical presentation, the principal differential diagnosis was myelopathy resulting from a congenital intramedullary vascular malformation, such as an arteriovenous malformation (AVM), centered at T11 to T12. Widespread congestion of the subarachnoid vascular bed was presumed to be a result of venous arterialization and vascular steal phenomenon.

Other differential diagnoses, underlying the production of an acquired arteriovenous fistula, were considered less likely based on the signalment but included vascular hamartoma or primary intramedullary neoplasia (eg, nephroblastoma, lymphoma, ependymoma, glial tumor, hemangioma, hemangioblastoma).
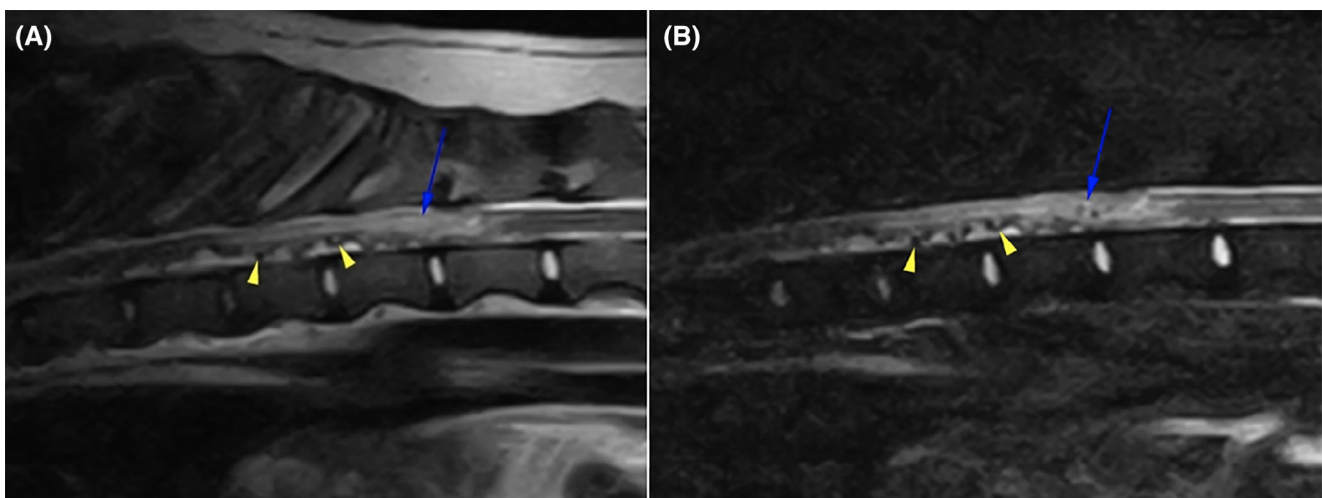

FIGURE 1   Sagittal T2-weighted, A, and sagittal short tau inversion recovery (STIR), B, magnetic resonance imaging (MRI) of the thoracic spinal cord. Distended subarachnoideal vessels can be seen as multifocal, tortuous, signal voiding, tubular structures extending throughout the subarachnoid space (arrowheads). The nidus-type arteriovenous malformation (AVM) is visible at the level of T11 to T12 vertebral bodies (arrow)

The more diffuse intramedullary T2W hyperintensity surrounding the primary lesion on MRI was considered to represent secondary perilesional spinal cord edema or gliosis, rather than extension of the primary pathology.

A T10 to T12 hemilaminectomy was performed in an attempt to surgically biopsy or excise the intramedullary lesion and explore options for surgical ligation or occlusion of any underlying AVM. Intraoperatively, an atrophic spinal cord wrapped in markedly distended subdural vessels was found. Because of the intramedullary nature of the principal lesion, the surgeon decided that resection or biopsy would be associated with a substantial risk of severe bleeding, and therefore such procedures were not attempted. The dog was conservatively treated with dexamethasone 0.2 mg/kg PO q24h postoperatively. Because of continued progression of the disease and loss of ability to ambulate independently 1 month after surgery, the owner elected euthanasia and consented to necropsy.

On necropsy, a focal, well-demarcated, dark red, soft, raised mass measuring approximately 1 cm in diameter and affecting the spinal cord at the level of T11 to T12 was found (Figure 3). The spinal cord

was immersed in a solution of 10% neutral buffered formalin, embedded in paraffin and multiple transverse sections were stained with hematoxylin and eosin. Macroscopic evaluation showed abundant, up to 4 mm (at their widest diameter), dilated and congested extramedullary blood vessels. On cross-sectional examination, the focal mass appeared to have extended into the spinal cord parenchyma and replaced parts of the gray and white matter (Figure 3).

Microscopic examination of the affected thoracic spinal cord identified diffusely dilated, tortuous and congested, dorsal and ventrally distributed, subdural and subarachnoideal venous plexuses. Focally, the macroscopically visible intradural glomus (focal mass) was composed of abnormal extramedullary and intramedullary patulous vessels with large lumens, common saccular dilatations, and often thickened venous walls with variable degrees of adventitial fibrosis (Figure 4). The arteriolar walls appeared thin and endothelial cells occasionally were swollen. The dilated, tortuous, and abnormal blood vessels were separated by spinal cord tissue that showed increased numbers of reactive glial cells, small areas of acute hemorrhages, and white matter degenerations. Caudal and cranial to this lesion, the
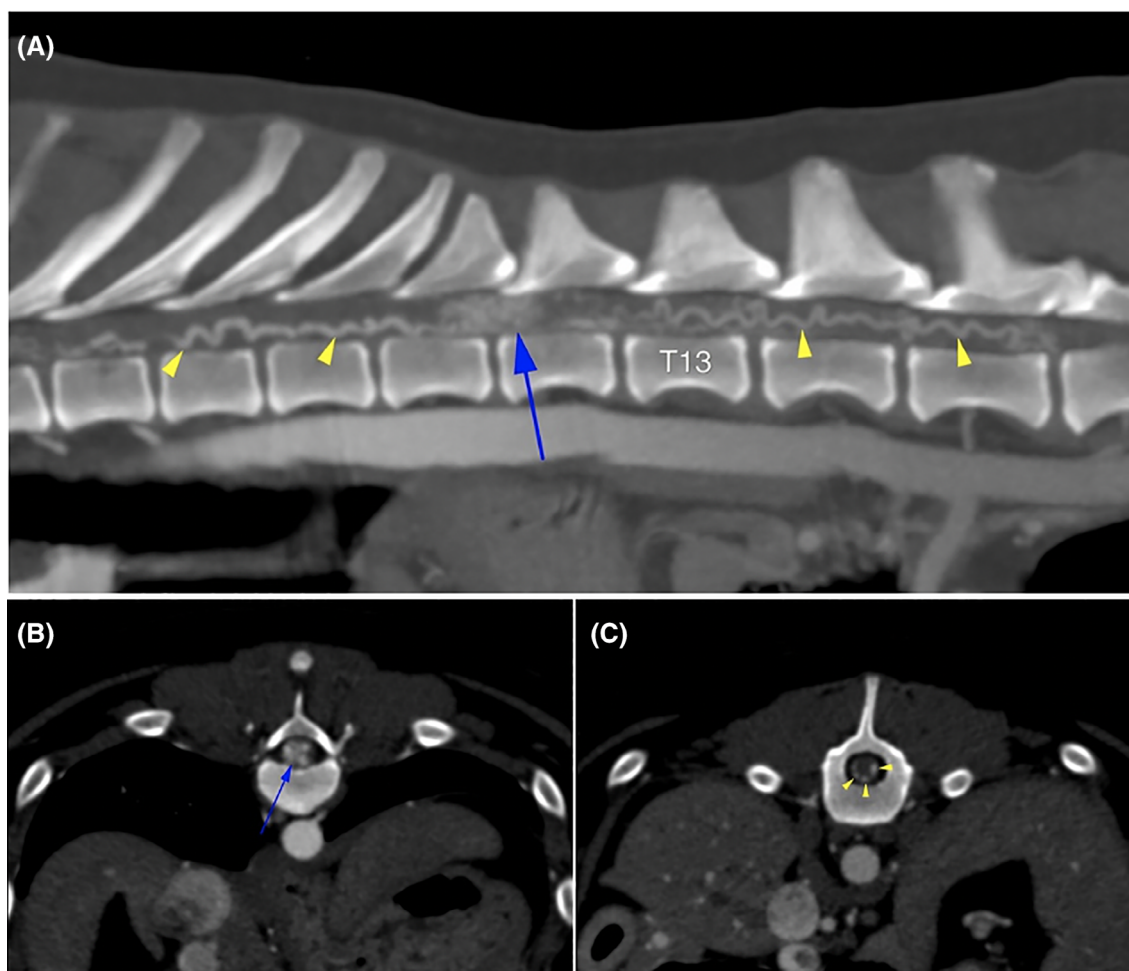

FIGURE 2 Sagittal, A, and transverse, B,C, reconstructions of a late arterial-phase computed tomography angiogram (CTA) of the thoracic spinal cord. Multiple, distended, tortuous, anastomosing, intradural extramedullary vessels are observed around the periphery of the spinal cord (arrowheads). An intramedullary focus at T11 to T12 represents a complex vascular plexus, formed of innumerable small anastomotic vessels, with strongest enhancement noted during the arterial phase (arrow)
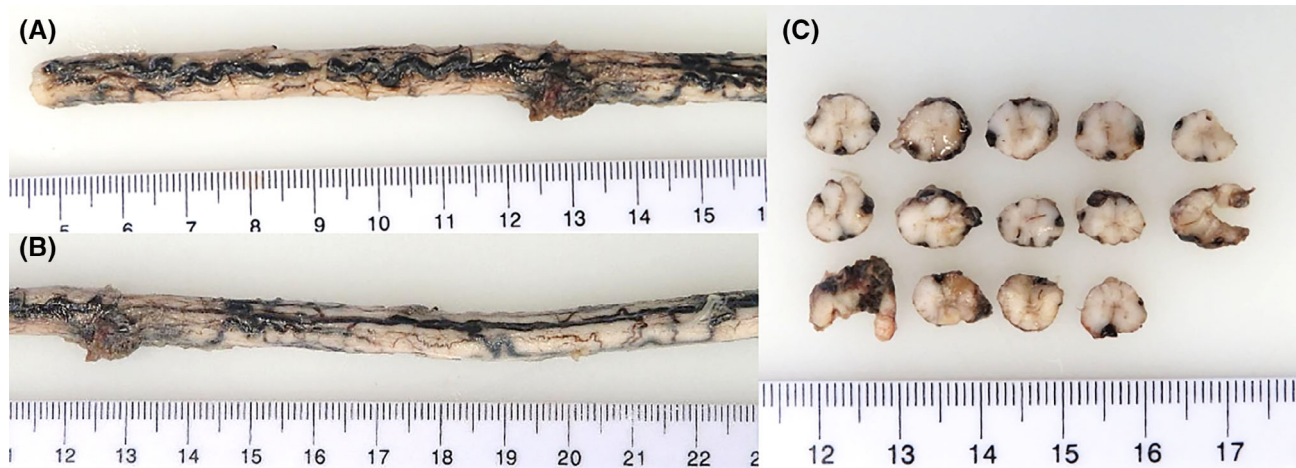
FIGURE 3 Macroscopic formalin fixed postmortem samples of the thoracic spinal cord, A,B, and transverse sections, C, of the same section of spinal cord. A focal, well demarcated, dark red, soft, raised mass was observed affecting the spinal cord at the level of T11 to T12 (A and B, at the levels 12-13 of the ruler). Macroscopic evaluation showed numerous, up to 4 mm diameter, dilated and congested extramedullary blood vessels. On cross sectional examination, this focal mass had extended into the spinal cord parenchyma, replacing large areas of both gray and white matter
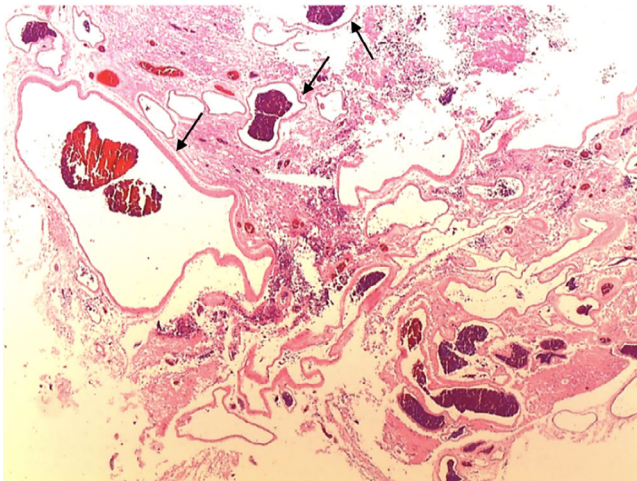

FIGURE 4 Histological section from the intradural glomus stained with hematoxylin and eosin. The glomus is composed of multiple, abnormal, intramedullary, and extramedullary distended vessels, with luminal enlargement, saccular dilations, and frequently thickened venous walls showing variable degrees of adventitial fibrosis (arrows)

subdural veins were markedly dilated. The histopathological diagnosis was consistent with diffuse venous and arterial congestion secondary to a focal intramedullary AVM.

2 | DISCUSSION

Vascular malformations affecting the spinal cord are rare in veterinary medicine, with only a few case reports in the literature.[1-16] In human medicine, the most widely accepted classification system divides vascular malformations of the central nervous system into 4 groups according to their histopathological features (Table 1): (a) capillary telangiectasia, (b) cavernous malformation, (c) venous angioma, and (d) AVM.[17,18]

Arteriovenous malformations are congenital abnormalities of the vasculature, in which a connection between the arterial and venous systems exists without an intervening capillary bed.[19] The result is chronic, high-flow, low-resistance, arteriovenous shunting, leading to dilatation of the congenitally normal feeding vessels and dilatation and hypertrophy of the draining veins.[18]

Neurological signs commonly are progressive and a consequence of venous congestion or hypertension, acute hemorrhage, compression from the chronically distended vessels, or vascular steal phenomenon.[20,21,22] This phenomenon occurs when high-flow shunting of blood through the AVM leads to deviation of the blood from the normal spinal cord circulation, ultimately resulting in decreased blood supply and ischemia of the surrounding neural tissue.[21-23]

In human medicine, different classification systems exist for spinal AVMs.[23-26] A widely accepted classification system divides AVMs into 6 different subtypes: (a) extradural arteriovenous fistulas; (b) intradural dorsal arteriovenous fistulas; (c) intradural ventral arteriovenous fistulas; (d) extradural-intradural AVMs; (e) intramedullary AVMs; and (f) conus medullaris AVMs.[27,28]

Our case resembles the intramedullary AVM lesions of humans, also called nidus-type, where 1 or multiple feeding vessels originating from spinal arteries form a compact intramedullary lesion, termed a glomus, with or without an extramedullary component, and drain into a venous plexus. These lesions typically are complex, characterized by high pressure and low resistance blood flow, and differ from arteriovenous shunts or fistulas where only a single direct connection between the arterial and venous circulation is present.[29]

Histopathologically, the nidus is composed of venous structures with collagenous walls and feeding arteries with muscular elastic walls.[18]

TABLE 1 Classification of malformations of the central nervous system[16,17]

Type of malformation	Other nomenclatures	Definition	Histological description
Capillary telangiectasia	Capillary angiomas; capillary malformation	Small, solitary, collections of dilated capillaries	Thin-walled, dilated capillaries lined by one layer of endothelial cells and devoid of smooth muscle and elastic fibers. Nervous tissue is typically present between the dilated capillaries
Cavernous malformation	Cavernous venous malformation; cavernoma; cavernous angioma	Solitary and circumscribed mass of vascular channels	Compact collection of large, sinusoidal, vascular spaces lined by one thin layer of endothelial cells devoid of smooth muscle and elastic fibers, and which are not separated by intervening nervous tissue. Minor to large hemorrhages frequently occur
Venous angioma	Venous malformation; Varix	Anomalous, dilated, veins	Thin-walled venous channels with walls composed of a single layer of fibromuscular tissue lined by a flat endothelium, devoid of smooth muscle and elastic fibers, and separated by intact neural parenchyma. The absence of arteries is necessary to reach a diagnosis
Arteriovenous malformation		Direct arterial-venous communications without intervening capillaries	Variable and complex depending on the subtype. Abnormal vessels ranging from relatively well-differentiated arteries and veins to malformed, thick or thin-walled, dilated vessels which neither be characterized as artery nor vein. The intervening neural parenchyma within the malformation is typically degenerated

To our knowledge, there are only 2 case reports of spinal AVMs in dogs. One case report describes a juvenile dog with a 3-week history of pelvic limb ataxia caused by an extramedullary and largely subdural AVM with epidural extension along the thoracolumbar spinal cord.[1] The second case report describes an intramedullary and leptomeningeal AVM in the cervical spinal cord of an adult dog with a 2-week history of right thoracic limb lameness, which rapidly progressed to right hemiplegia.[3] In both case reports, imaging studies were not performed and the final diagnosis was achieved postmortem, by means of histopathology. Ours represent the first case report of an intramedullary spinal AVM in a dog documented antemortem, based on findings of MRI and CTA.

In human medicine, the diagnosis of spinal AVMs typically is achieved in 2 steps. First, a screening study is performed to investigate the cause of myelopathy. This screening then is followed by a vascular imaging study to confirm the diagnosis, characterize the anatomical anomaly present, and guide treatment.[27]

High-field MRI is considered the gold standard screening method because it is noninvasive and provides a diagnosis of AVM.[30]

The MRI findings of intramedullary AVMs include: (a) a focal, intramedullary cluster of signal voids in T1-weighted images, causing focal expansion of the spinal cord; (b) abnormal vessels in the subarachnoid space, characterized by a serpentine pattern of low signal on T1W and T2W imaging, that represent the dilated, tortuous, arterialized pial veins; (c) local intramedullary signal changes secondary to venous congestion, myelomalacia, edema, ischemia, hemorrhage, or some combination of these and, (d) subacute hemorrhages that may or may not be present and are represented by increased signal on T1W images.[30-32]

Our case had similar findings to those reported in the human literature, with the nidus located at the level of the T11 to T12 spinal cord

segment and evidence of marked venous distension and congestion along the subarachnoid space after arterialization of the venous system. The high signal of the intramedullary lesion on T1W images likely was a result of hemorrhage,[30] as observed during histopathologic examination. The lack of susceptibility artifact on T2*W GRE images associated with this lesion is suspected to be a result of the combination of low-field strength and the scant amount of hemorrhage.

In recent years, magnetic resonance angiography (MRA), including both time-resolved spinal MRA and contrast-enhanced MRA, has been shown to provide additional information regarding the type of malformation present.[33,34] These images are advantageous to guide subsequent spinal digital subtraction arteriography, markedly decreasing the amount of time and contrast media required during the procedure.[34,35] Unfortunately, limitations surrounding MRA at our institution precluded use of this technique in our patient.

Computed tomography generally is inferior to MRI for investigation into causes of myelopathy, but has considerable advantages, including shorter acquisition times with increased spatial resolution and scanning range.[36] In addition, CTA may successfully allow diagnosis of spinal AVMs by identifying the feeding arteries and draining veins.[37,38]

In our case, CTA confirmed the suspicion of arteriovenous shunting by identifying contrast uptake in the arterialized venous system during the arterial phase. Because of the limited spatial and temporal resolution of the CT machine used, the specific feeding artery or arteries could not be identified.

Digital spinal arteriography is considered the gold standard diagnostic imaging technique for spinal AVMs. It offers high spatial and temporal resolution and provides detailed anatomical information to facilitate endovascular treatment, including the type and exact location of the malformation,[30,39] the anatomical characteristics of the

nidus, identification of the feeding arteries, and a detailed understanding of the normal vascular anatomy of the spinal cord. [40,41]

In human medicine, untreated spinal AVMs are associated with a poor prognosis, therefore, aggressive intervention is advised. [42] The ultimate goal of treatment is complete and permanent obliteration of the AVM, while preserving adequate blood supply to the spinal cord. [40]

Several treatment modalities have been described for intramedullary AVMs including microsurgical resection, [43] endovascular embolization, [44] and radiation treatment, [45] as well as a combination of these procedures. With respect to the different outcomes reported with these treatments, the gold standard of treatment is debatable, with some authors reporting successful outcomes using endovascular treatment alone, and others reporting the need for microsurgical resection as a first-line treatment or after endovascular treatment, depending on the size of the lesion. [45-47] In cases where lesions are large in size, involve the ventral half of the spinal cord, or involve multiple feeding vessels from the anterior spinal artery, definitive treatment is not feasible without substantial neurological dysfunction and iatrogenic disability postoperatively. [43,44,48]

In our case, the intramedullary location and size of the lesion precluded surgical resection. Considering the microscopic size of the vessels involved, endovascular treatment was not feasible.

3 | SUMMARY

Congenital vascular malformations should be considered as a differential diagnosis in young dogs presented with signs of progressive myelopathy. Visualization of an intramedullary lesion associated with diffuse venous distension should increase suspicion for arterialization of the venous system and underlying arteriovenous shunting.

CONFLICT OF INTEREST DECLARATION
Authors declare no conflict of interest.

OFF-LABEL ANTIMICROBIAL DECLARATION
Authors declare no off-label use of antimicrobials.

INSTITUTIONAL ANIMAL CARE AND USE COMMITTEE (IACUC) OR OTHER APPROVAL DECLARATION
Authors declare no IACUC or other approval was needed.

HUMAN ETHICS APPROVAL DECLARATION
Authors declare human ethics approval was not needed for this study.

ORCID
Maria Ines De Freitas https://orcid.org/0000-0003-1531-3280

REFERENCES
1. Cordy DR. Vascular malformations and hemangiomas of the canine spinal cord. *Vet Pathol*. 1979;6:275-282.
2. Zaki FA. Vascular malformation (cavernous angioma) of the spinal cord in a dog. *J Small Anim Pract*. 1979;20:417-422.
3. Hayashida E, Ochiai K, Kadosawa T, et al. Arteriovenous malformation of the cervical spinal cord in a dog. *J Comp Pathol*. 1999;121:71-76.
4. Sanders SG, Bagley RS, Gavin PR, et al. Surgical treatment of an intramedullary spinal cord hamartoma in a dog. *J Am Vet Med Assoc*. 2002; 221:659-661.
5. Westworth DR, Vernau KM, Cullen SP, et al. Vascular anomaly causing subclavian steal and cervical myelopathy in a dog: diagnosis and endovascular management. *Vet Radiol Ultrasound*. 2006;47:265-269.
6. MacKillop E, Olby NJ, Linder KE, et al. Intramedullary cavernous malformation of the spinal cord in two dogs. *Vet Pathol*. 2007;44: 528-532.
7. Alexander K, Huneault L, Foster R, et al. Magnetic resonance imaging and marsupialization of a hemorrhagic intramedullary vascular anomaly in the cervical portion of the spinal cord of a dog. *J Am Vet Med Assoc*. 2008;232:399-404.
8. Jull P, Walmsley GL, Benigni L, et al. Spinal cord hemangioma in two dogs. *Veterinary Radiol Ultrasound*. 2011;52:653-657.
9. Bozynski CC, Vasquez L, O'Brien DP, et al. Compressive myelopathy associated with ectasia of the vertebral and spinal arteries in a dog. *Vet Pathol*. 2012;49:779.
10. Morabito S, Auriemma E, Zagarella P, et al. Computed tomographic and angiographic assessment of spinal extradural arteriovenous fistulas in a dog. *Can Vet J*. 2017;58:275-279.
11. Westworth DR, Sturges BK. Congenital spinal malformations in small animals. *Vet Clin North America Small Anim Pract*. 2010;40:951-981.
12. Westworth DR, Vernau KM, Lecouteur RA, et al. Definitive follow up on an arterial anomaly causing cervical myelopathy. *Vet Radiol Ultrasound*. 2010;51:356-357.
13. Cho DY, Cook JE, Leipold HW. Angiomatous vascular malformation in the spinal cord of a Hereford calf. *Vet Pathol*. 1979;16:613-616.
14. Gilmour JS, Fraser JA. Ataxia in a Welsh cob filly due to a venous malformation in the thoracic spinal cord. *Equine Vet J*. 1977;9:40-42.
15. Palmer AC, Hickman J. Ataxia in a horse due to an angioma of the spinal cord. *Vet Rec*. 1960;72:611-613.
16. Vandevelde M, Frankenhauser R. Zur Pathologie der Ruckenmarksblutungen beim Hund. *Schweiz Arch Tierheilkd*. 1972; 114:463-475.
17. McCormick WF. The pathology of vascular ("arteriovenous") malformations. *J Neurosurg*. 1966;24:807-816.
18. Jellinger K. Vascular malformations of the central nervous system: a morphological overview. *Neurosurg Rev*. 1986;9(3):177-216.
19. Krings T. Vascular malformations of the spine and spinal cord: anatomy, classification, treatment. *Clin Neuroradiol*. 2010;20:5-24.
20. Sood D, Mistry KA, Khatri GD, et al. Congestive myelopathy due to intradural spinal AVM supplied by artery of Adamkiewicz: case report with brief literature review and analysis of the Foix-Alajouanine syndrome definition. *Pol J Radiol*. 2015;80:337-343.
21. Aminoff MJ, Barnard RO, Logue V. The pathophysiology of spinal vascular malformations. *J Neural Sci*. 1974;23:255-263.
22. Jahan R, Vinuela F. Vascular anatomy, pathophysiology, and classification of vascular malformations of the spinal cord. *Sem Cerebrovasc Dis Stroke*. 2002;2(3):190–192.
23. Rosenblum B, Oldfield EH, Doppman JL, et al. Spinal arteriovenous malformations: a comparison of dural arteriovenous fistulas and intradural AVM's in 81 patients. *J Neurosurg*. 1987;67:795-802.
24. Bao YH, Ling F. Classification and therapeutic modalities of spinal vascular malformations in 80 patients. *Neurosurgery*. 1997;40:75-81.
25. Di Chiro G, Doppman J, Ommaya AK. Selective arteriography of arteriovenous aneurysms of spinal cord. *Radiology*. 1967;88:1065-1077.
26. TaKai K. Spinal Arteriovenous shunts: angioarchitecture and historical changes in classification. *Neurol Med Chir (Tokyo)*. 2017;57:356-365.
27. Winn HR, Youmans JYR. *Winn Neurological Surgery*. 6th ed. Philadelphia, PA: Elsevier; 2017:4167–4189.

28. Kim LJ, Spetzler RF. Classification and surgical management of spinal arteriovenous lesions: arteriovenous fistulae and arteriovenous malformations. *Neurosurgery*. 2006;59(5 suppl 3):S195-S201.

29. Spetzler RF, Detwiler PW, Riina HA, et al. Modified classification of spinal cord vascular lesions. *J Neurosurg*. 2002;96(suppl 2):145-156.

30. Krings T, Lasjaunias PL, Hans FJ, et al. Imaging in spinal vascular disease. *Neuroimag Clin N Am*. 2007;17:57-72.

31. Doppman JL, Di Chiro G, Dwyer AJ, et al. Magnetic resonance imaging of spinal arteriovenous malformations. *J Neurosurg*. 1987;66(6):830-834.

32. DiChiro G, Doppman JL, Dwyer AJ, et al. Tumors and arteriovenous malformations of the spinal cord: assessment using MR. *Radiology*. 1985;156:689-697.

33. Mull M, Nijenhuis RJ, Backes WH, et al. Value and limitations of contrast-enhanced MR angiography in spinal arteriovenous malformations and dural arteriovenous fistulas. *Am J Neuroradiol*. 2007;28:1249-1258.

34. Cao JB, Cui LL, Jiang XY, et al. Clinical application and diagnostic value of noninvasive spinal angiography in spinal vascular malformations. *J Comput Assist Tomogr*. 2014;38:474-479.

35. Luetmer PH, Lane JI, Gilbertson JR, et al. Preangiographic evaluation of spinal dural arteriovenous fistulas with elliptic centric contrast-enhanced MR angiography and effect on radiation dose and volume of iodinated contrast material. *Am J Neuroradiol*. 2005;26:711-718.

36. Cooper JJ, Young BD, Griffin JF IV, et al. Comparison between non-contrast computed tomography and magnetic resonance imaging for detection and characterization of thoracolumbar myelopathy caused by intervertebral disk herniation in dogs. *Vet Radiol Ultrasound*. 2014;55(2):182-189.

37. Si-jia G, Meng-wei Z, Xi-ping L, et al. The clinical application studies of CT spinal angiography with 64-detector row spiral CT in diagnosing spinal vascular malformations. *Eur J Radiol*. 2009;71(1):22-28.

38. Yamaguchi S, Eguchi K, Kiura Y, et al. Multi-detector-row CT angiography as a preoperative evaluation for spinal arteriovenous fistulae. *Neurosurg Rev*. 2007;30:321-327.

39. Rodesch G, Lasjaunias P. Spinal cord arteriovenous shunts: from imaging to management. *Eur J Radiol*. 2003;46:221-232.

40. McDougall CG, Deshmukh VR, Fiorella DJ, et al. Endovascular techniques for vascular malformations of the spinal axis. *Neurosurg Clin N Am*. 2005;16:395-410.

41. Matsubara N, Miyachi S, Izumi T, et al. Usefulness of three-dimensional digital subtraction angiography in endovascular treatment of a spinal dural arteriovenous fistula. *J Neurosurg Spine*. 2008;8:462-467.

42. Aminoff MJ, Logue V. The prognosis of patients with spinal vascular malformations. *Brain*. 1974;97:211-218.

43. Boström A, Krings T, Hans FJ, et al. Spinal glomus-type arteriovenous malformations: microsurgical treatment in 20 cases. *J Neurosurg Spine*. 2009;10:423-429.

44. Krings T, Thron AK, Geibprasert S, et al. Endovascular management of spinal vascular malformations. *Neurosurg Rev*. 2010;33:1-9.

45. Ryu SI, Chang SD, Kim DH, et al. Image-guided hypo-fractionated stereotactic radiosurgery to spinal lesions. *Neurosurgery*. 2001;49:838-846.

46. Gross BA, Albuquerque FC, Moon K, et al. Validation of an "endovascular-first" approach to spinal dural arteriovenous fistulas: an intention-to-treat analysis. *J Neurointerv Surg*. 2017;9:102-105.

47. Rangel-Castilla L, Russin JJ, Zaidi HA, et al. Contemporary management of spinal AVFs and AVMs: lessons learned from 110 cases. *Neurosurg Focus*. 2014;37(3):E14.

48. Ye ZP, Yang XY, Li WS, et al. Microsurgical resection of cervical spinal cord arteriovenous malformations: report of 6 cases. *World Neurosurg*. 2016;96:362-336.